BELLE-CONF-0475
Contributed to FPCP2004

New Measurements of Time-Dependent CP-Violating Asymmetries in $B^0 \to K^0_S K^0_S K^0_S$ and $K^0_S \pi^0 \gamma$ Decays at Belle

K. Abe,[10] K. Abe,[46] N. Abe,[49] I. Adachi,[10] H. Aihara,[48] M. Akatsu,[24] Y. Asano,[53] T. Aso,[52] V. Aulchenko,[2] T. Aushev,[14] T. Aziz,[44] S. Bahinipati,[6] A. M. Bakich,[43] Y. Ban,[36] M. Barbero,[9] A. Bay,[20] I. Bedny,[2] U. Bitenc,[15] I. Bizjak,[15] S. Blyth,[29] A. Bondar,[2] A. Bozek,[30] M. Bračko,[22,15] J. Brodzicka,[30] T. E. Browder,[9] M.-C. Chang,[29] P. Chang,[29] Y. Chao,[29] A. Chen,[26] K.-F. Chen,[29] W. T. Chen,[26] B. G. Cheon,[4] R. Chistov,[14] S.-K. Choi,[8] Y. Choi,[42] Y. K. Choi,[42] A. Chuvikov,[37] S. Cole,[43] M. Danilov,[14] M. Dash,[55] L. Y. Dong,[12] R. Dowd,[23] J. Dragic,[23] A. Drutskoy,[6] S. Eidelman,[2] Y. Enari,[24] D. Epifanov,[2] C. W. Everton,[23] F. Fang,[9] S. Fratina,[15] H. Fujii,[10] N. Gabyshev,[2] A. Garmash,[37] T. Gershon,[10] A. Go,[26] G. Gokhroo,[44] B. Golob,[21,15] M. Grosse Perdekamp,[38] H. Guler,[9] J. Haba,[10] F. Handa,[47] K. Hara,[10] T. Hara,[34] N. C. Hastings,[10] K. Hasuko,[38] K. Hayasaka,[24] H. Hayashii,[25] M. Hazumi,[10] E. M. Heenan,[23] I. Higuchi,[47] T. Higuchi,[10] L. Hinz,[20] T. Hojo,[34] T. Hokuue,[24] Y. Hoshi,[46] K. Hoshina,[51] S. Hou,[26] W.-S. Hou,[29] Y. B. Hsiung,[29] H.-C. Huang,[29] T. Igaki,[24] Y. Igarashi,[10] T. Iijima,[24] A. Imoto,[25] K. Inami,[24] A. Ishikawa,[10] H. Ishino,[49] K. Itoh,[48] R. Itoh,[10] M. Iwamoto,[3] M. Iwasaki,[48] Y. Iwasaki,[10] R. Kagan,[14] H. Kakuno,[48] J. H. Kang,[56] J. S. Kang,[17] P. Kapusta,[30] S. U. Kataoka,[25] N. Katayama,[10] H. Kawai,[3] H. Kawai,[48] Y. Kawakami,[24] N. Kawamura,[1] T. Kawasaki,[32] N. Kent,[9] H. R. Khan,[49] A. Kibayashi,[49] H. Kichimi,[10] H. J. Kim,[19] H. O. Kim,[42] Hyunwoo Kim,[17] J. H. Kim,[42] S. K. Kim,[41] T. H. Kim,[56] K. Kinoshita,[6] P. Koppenburg,[10] S. Korpar,[22,15] P. Križan,[21,15] P. Krokovny,[2] R. Kulasiri,[6] C. C. Kuo,[26] H. Kurashiro,[49] E. Kurihara,[3] A. Kusaka,[48] A. Kuzmin,[2] Y.-J. Kwon,[56] J. S. Lange,[7] G. Leder,[13] S. E. Lee,[41] S. H. Lee,[41] Y.-J. Lee,[29] T. Lesiak,[30] J. Li,[40] A. Limosani,[23] S.-W. Lin,[29] D. Liventsev,[14] J. MacNaughton,[13] G. Majumder,[44] F. Mandl,[13] D. Marlow,[37] T. Matsuishi,[24] H. Matsumoto,[32] S. Matsumoto,[5] T. Matsumoto,[50] A. Matyja,[30] Y. Mikami,[47] W. Mitaroff,[13] K. Miyabayashi,[25] Y. Miyabayashi,[24] H. Miyake,[34] H. Miyata,[32] R. Mizuk,[14] D. Mohapatra,[55] G. R. Moloney,[23] G. F. Moorhead,[23] T. Mori,[49] A. Murakami,[39] T. Nagamine,[47] Y. Nagasaka,[11] T. Nakadaira,[48] I. Nakamura,[10] E. Nakano,[33] M. Nakao,[10] H. Nakazawa,[10] Z. Natkaniec,[30] K. Neichi,[46] S. Nishida,[10] O. Nitoh,[51] S. Noguchi,[25] T. Nozaki,[10] A. Ogawa,[38] S. Ogawa,[45] T. Ohshima,[24] T. Okabe,[24] S. Okuno,[16] S. L. Olsen,[9] Y. Onuki,[32] W. Ostrowicz,[30] H. Ozaki,[10] P. Pakhlov,[14] H. Palka,[30] C. W. Park,[42] H. Park,[19] K. S. Park,[42] N. Parslow,[43] L. S. Peak,[43] M. Pernicka,[13] J.-P. Perroud,[20] M. Peters,[9] L. E. Piilonen,[55] A. Poluektov,[2] F. J. Ronga,[10] N. Root,[2] M. Rozanska,[30] H. Sagawa,[10] M. Saigo,[47] S. Saitoh,[10] Y. Sakai,[10] H. Sakamoto,[18] T. R. Sarangi,[10] M. Satapathy,[54] N. Sato,[24] O. Schneider,[20] J. Schümann,[29] C. Schwanda,[13] A. J. Schwartz,[6] T. Seki,[50] S. Semenov,[14] K. Senyo,[24] Y. Settai,[5] R. Seuster,[9] M. E. Sevior,[23] T. Shibata,[32] H. Shibuya,[45] B. Shwartz,[2] V. Sidorov,[2] V. Siegle,[38] J. B. Singh,[35] A. Somov,[6] N. Soni,[35] R. Stamen,[10] S. Stanič,[53,*] M. Starič,[15] A. Sugi,[24] A. Sugiyama,[39] K. Sumisawa,[34] T. Sumiyoshi,[50] S. Suzuki,[39] S. Y. Suzuki,[10] O. Tajima,[10] F. Takasaki,[10] K. Tamai,[10] N. Tamura,[32] K. Tanabe,[48] M. Tanaka,[10] G. N. Taylor,[23]

Y. Teramoto,[33] X. C. Tian,[36] S. Tokuda,[24] S. N. Tovey,[23] K. Trabelsi,[9] T. Tsuboyama,[10] T. Tsukamoto,[10] K. Uchida,[9] S. Uehara,[10] T. Uglov,[14] K. Ueno,[29] Y. Unno,[3] S. Uno,[10] Y. Ushiroda,[10] G. Varner,[9] K. E. Varvell,[43] S. Villa,[20] C. C. Wang,[29] C. H. Wang,[28] J. G. Wang,[55] M.-Z. Wang,[29] M. Watanabe,[32] Y. Watanabe,[49] L. Widhalm,[13] Q. L. Xie,[12] B. D. Yabsley,[55] A. Yamaguchi,[47] H. Yamamoto,[47] S. Yamamoto,[50] T. Yamanaka,[34] Y. Yamashita,[31] M. Yamauchi,[10] Heyoung Yang,[41] P. Yeh,[29] J. Ying,[36] K. Yoshida,[24] Y. Yuan,[12] Y. Yusa,[47] H. Yuta,[1] S. L. Zang,[12] C. C. Zhang,[12] J. Zhang,[10] L. M. Zhang,[40] Z. P. Zhang,[40] V. Zhilich,[2] T. Ziegler,[37] D. Žontar,[21,15] and D. Zürcher[20]

(The Belle Collaboration)

[1]*Aomori University, Aomori*
[2]*Budker Institute of Nuclear Physics, Novosibirsk*
[3]*Chiba University, Chiba*
[4]*Chonnam National University, Kwangju*
[5]*Chuo University, Tokyo*
[6]*University of Cincinnati, Cincinnati, Ohio 45221*
[7]*University of Frankfurt, Frankfurt*
[8]*Gyeongsang National University, Chinju*
[9]*University of Hawaii, Honolulu, Hawaii 96822*
[10]*High Energy Accelerator Research Organization (KEK), Tsukuba*
[11]*Hiroshima Institute of Technology, Hiroshima*
[12]*Institute of High Energy Physics, Chinese Academy of Sciences, Beijing*
[13]*Institute of High Energy Physics, Vienna*
[14]*Institute for Theoretical and Experimental Physics, Moscow*
[15]*J. Stefan Institute, Ljubljana*
[16]*Kanagawa University, Yokohama*
[17]*Korea University, Seoul*
[18]*Kyoto University, Kyoto*
[19]*Kyungpook National University, Taegu*
[20]*Swiss Federal Institute of Technology of Lausanne, EPFL, Lausanne*
[21]*University of Ljubljana, Ljubljana*
[22]*University of Maribor, Maribor*
[23]*University of Melbourne, Victoria*
[24]*Nagoya University, Nagoya*
[25]*Nara Women's University, Nara*
[26]*National Central University, Chung-li*
[27]*National Kaohsiung Normal University, Kaohsiung*
[28]*National United University, Miao Li*
[29]*Department of Physics, National Taiwan University, Taipei*
[30]*H. Niewodniczanski Institute of Nuclear Physics, Krakow*
[31]*Nihon Dental College, Niigata*
[32]*Niigata University, Niigata*
[33]*Osaka City University, Osaka*
[34]*Osaka University, Osaka*
[35]*Panjab University, Chandigarh*
[36]*Peking University, Beijing*

[37]Princeton University, Princeton, New Jersey 08545
[38]RIKEN BNL Research Center, Upton, New York 11973
[39]Saga University, Saga
[40]University of Science and Technology of China, Hefei
[41]Seoul National University, Seoul
[42]Sungkyunkwan University, Suwon
[43]University of Sydney, Sydney NSW
[44]Tata Institute of Fundamental Research, Bombay
[45]Toho University, Funabashi
[46]Tohoku Gakuin University, Tagajo
[47]Tohoku University, Sendai
[48]Department of Physics, University of Tokyo, Tokyo
[49]Tokyo Institute of Technology, Tokyo
[50]Tokyo Metropolitan University, Tokyo
[51]Tokyo University of Agriculture and Technology, Tokyo
[52]Toyama National College of Maritime Technology, Toyama
[53]University of Tsukuba, Tsukuba
[54]Utkal University, Bhubaneswer
[55]Virginia Polytechnic Institute and State University, Blacksburg, Virginia 24061
[56]Yonsei University, Seoul

(Dated: February 7, 2008)

Abstract

We present new measurements of CP-violation parameters in $B^0 \to K^0_S K^0_S K^0_S$ and $K^0_S \pi^0 \gamma$ decays based on a sample of 275×10^6 $B\overline{B}$ pairs collected at the $\Upsilon(4S)$ resonance with the Belle detector at the KEKB energy-asymmetric e^+e^- collider. One neutral B meson is fully reconstructed in one of the specified decay channels, and the flavor of the accompanying B meson is identified from its decay products. CP-violation parameters are obtained from the asymmetries in the distributions of the proper-time intervals between the two B decays. We obtain

$$\begin{aligned}
\mathcal{S}_{K^0_S K^0_S K^0_S} &= +1.26 \pm 0.68(\text{stat}) \pm 0.18(\text{syst}), \\
\mathcal{A}_{K^0_S K^0_S K^0_S} &= +0.54 \pm 0.34(\text{stat}) \pm 0.08(\text{syst}), \\
\mathcal{S}_{K^0_S \pi^0 \gamma} &= -0.58^{+0.46}_{-0.38}(\text{stat}) \pm 0.11(\text{syst}), \\
\mathcal{A}_{K^0_S \pi^0 \gamma} &= +0.03 \pm 0.34(\text{stat}) \pm 0.11(\text{syst}).
\end{aligned}$$

All results are preliminary.

PACS numbers: 11.30.Er, 12.15.Hh, 13.25.Hw

*on leave from Nova Gorica Polytechnic, Nova Gorica

I. INTRODUCTION

In the standard model (SM), CP violation arises from an irreducible phase, the Kobayashi-Maskawa (KM) phase [1], in the weak-interaction quark-mixing matrix. In particular, the SM predicts CP asymmetries in the time-dependent rates for B^0 and $\overline{B}^0$ decays to a common CP eigenstate f_{CP} [2]. In the decay chain $\Upsilon(4S) \to B^0\overline{B}^0 \to f_{CP}f_{\rm tag}$, where one of the B mesons decays at time t_{CP} to a final state f_{CP} and the other decays at time $t_{\rm tag}$ to a final state $f_{\rm tag}$ that distinguishes between B^0 and $\overline{B}^0$, the decay rate has a time dependence given by

$$\mathcal{P}(\Delta t) = \frac{e^{-|\Delta t|/\tau_{B^0}}}{4\tau_{B^0}}\Big\{1 + q\cdot\Big[\mathcal{S}\sin(\Delta m_d\Delta t) + \mathcal{A}\cos(\Delta m_d\Delta t)\Big]\Big\}. \quad (1)$$

Here $\mathcal{S}$ and $\mathcal{A}$ are CP-violation parameters, τ_{B^0} is the B^0 lifetime, Δm_d is the mass difference between the two B^0 mass eigenstates, $\Delta t = t_{CP} - t_{\rm tag}$, and the b-flavor charge $q = +1$ (-1) when the tagging B meson is a B^0 ($\overline{B}^0$). To a good approximation, the SM predicts $\mathcal{S} = -\xi_f \sin 2\phi_1$, where $\xi_f = +1(-1)$ corresponds to CP-even (-odd) final states, and $\mathcal{A} = 0$ for both $b \to c\overline{c}s$ and $b \to s\overline{q}q$ transitions. Recent measurements of time-dependent CP asymmetries in $B^0 \to J/\psi K^0_S$ [3] and related decay modes, which are governed by the $b \to c\overline{c}s$ transition, by Belle [4, 5] and BaBar [6] already determine $\sin 2\phi_1$ rather precisely; the present world average value is $\sin 2\phi_1 = +0.726\pm0.037$ [7]. This serves as a firm reference point for the SM.

The phenomena of CP violation in the flavor-changing $b \to s$ transition are sensitive to physics at a very high-energy scale [8]. Theoretical studies indicate that large deviations from SM expectations are allowed for time-dependent CP asymmetries in B^0 meson decays [9]. Experimental investigations have recently been launched at the two B factories, each of which has produced more than 10^8 $B\overline{B}$ pairs. Belle's measurements of CP asymmetries using the decay modes $B^0 \to \phi K^0_S$, ϕK^0_L, $K^+K^-K^0_S$, $f_0(980)K^0_S$, $\eta' K^0_S$, ωK^0_S, and $K^0_S\pi^0$, which are dominated by the $b \to s\overline{q}q$ transition, yielded a value that differs from the SM expectation by 2.4 standard deviations when all measurements are combined [10]. To elucidate the difference, it is essential to examine additional modes that may be sensitive to the same $b \to s$ penguin amplitude.

Recently it was pointed out that in decays of the type $B^0 \to P^0Q^0X^0$, where P^0, Q^0 and X^0 represent spin-0 neutral particles that are CP eigenstates, the final state is a CP eigenstate [11]. The $B^0 \to K^0_SK^0_SK^0_S$ decay, which is a $\xi_f = +1$ state, is one of the most promising modes in this class of decays. The existence of this decay mode was first reported by the Belle collaboration [12], and recently confirmed with larger statistics by the BaBar collaboration [13]. Since there is no u quark in the final state, the decay is dominated by the $b \to s\overline{s}s$ transition. In this report, we describe the first measurement of CP asymmetries in the $B^0 \to K^0_SK^0_SK^0_S$ decay based on a 253 fb^{-1} data sample that contains 275×10^6 $B\overline{B}$ pairs.

We also measure time-dependent CP violation in the decay $B^0 \to K^0_S\pi^0\gamma$, which is not a CP eigenstate but is sensitive to physics beyond the SM [14, 15]. Within the SM, the photon emitted from a B^0 ($\overline{B}^0$) meson is dominantly right-handed (left-handed). Therefore the polarization of the photon carries information on the original b-flavor; the decay is thus almost flavor-specific. The SM predicts a small asymmetry $\mathcal{S} \sim -2(m_s/m_b)\sin 2\phi_1$, where m_b (m_s) is the b-quark (s-quark) mass [15]. Any significant deviation from this expectation would be a manifestation of physics beyond the SM. Belle's previous measurement of time-dependent CP asymmetries in the decay $B^0 \to K^{*0}\gamma$ ($K^{*0} \to K^0_S\pi^0$) [10] required that

the invariant mass of the K^0_S and π^0 ($M_{K^0_S\pi^0}$) be between 0.8 and 1.0 GeV/c^2 to select the $K^{*0} \to K^0_S\pi^0$ decay [14]. Recently it was pointed out that in decays of the type $B^0 \to P^0Q^0\gamma$ (e.g. $P^0 = K^0_S$ and $Q^0 = \pi^0$), possible new physics effects on the mixing-induced CP violation do not depend on the resonant structure of the P^0Q^0 system [15]. In this report, we describe a new measurement of CP asymmetries extending the invariant mass range to $0.6 < M_{K^0_S\pi^0} < 1.8$ GeV/c^2, which includes the K^{*0} mass region, based on the new proposal.

At the KEKB energy-asymmetric e^+e^- (3.5 on 8.0 GeV) collider [16], the $\Upsilon(4S)$ is produced with a Lorentz boost of $\beta\gamma = 0.425$ nearly along the electron beamline (z). Since the B^0 and $\overline{B}^0$ mesons are approximately at rest in the $\Upsilon(4S)$ center-of-mass system (cms), Δt can be determined from the displacement in z between the f_{CP} and $f_{\rm tag}$ decay vertices: $\Delta t \simeq (z_{CP} - z_{\rm tag})/(\beta\gamma c) \equiv \Delta z/(\beta\gamma c)$.

The Belle detector is a large-solid-angle magnetic spectrometer that consists of a silicon vertex detector (SVD), a 50-layer central drift chamber (CDC), an array of aerogel threshold Cherenkov counters (ACC), a barrel-like arrangement of time-of-flight scintillation counters (TOF), and an electromagnetic calorimeter comprised of CsI(Tl) crystals (ECL) located inside a superconducting solenoid coil that provides a 1.5 T magnetic field. An iron flux-return located outside of the coil is instrumented to detect K^0_L mesons and to identify muons (KLM). The detector is described in detail elsewhere [17]. Two inner detector configurations were used. A 2.0 cm radius beampipe and a 3-layer silicon vertex detector (SVD-I) were used for a 140 fb^{-1} data sample (DS-I) containing 152×16^6 $B\overline{B}$ pairs, while a 1.5 cm radius beampipe, a 4-layer silicon detector (SVD-II) [18] and a small-cell inner drift chamber were used for an additional 113 fb^{-1} data sample (DS-II) that contains 123×10^6 $B\overline{B}$ pairs for a total of 275×10^6 $B\overline{B}$ pairs.

II. EVENT SELECTION, FLAVOR TAGGING AND VERTEX RECONSTRUCTION

A. $B^0 \to K^0_S K^0_S K^0_S$

We reconstruct the $B^0 \to K^0_S K^0_S K^0_S$ decay with a $K^{+-}_S K^{+-}_S K^{+-}_S$ or $K^{+-}_S K^{+-}_S K^{00}_S$ final state, where a $\pi^+\pi^-$ ($\pi^0\pi^0$) state from a K^0_S decay is denoted as K^{+-}_S (K^{00}_S). We use these notations whenever appropriate. Although the $K^{+-}_S K^{+-}_S K^{00}_S$ state suffers from a larger background and a lower vertex reconstruction efficiency, we include it because its total branching fraction is larger than that of the $K^{+-}_S K^{+-}_S K^{+-}_S$ mode; with $\mathcal{B}(K^0_S \to \pi^+\pi^-) = 2/3$ and $\mathcal{B}(K^0_S \to \pi^0\pi^0) = 1/3$, we obtain $\mathcal{B}(3K^0_S \to K^{+-}_S K^{+-}_S K^{+-}_S) = (2/3)^3 = 8/27$ while $\mathcal{B}(3K^0_S \to K^{+-}_S K^{+-}_S K^{00}_S) = 3(2/3)^2(1/3) = 12/27$. We do not include final states with two or three $K^0_S \to \pi^0\pi^0$ since their products of efficiencies and branching fractions are small.

Pairs of oppositely charged tracks that have an invariant mass within 0.012 GeV/c^2 of the nominal K^0_S mass are used to reconstruct $K^0_S \to \pi^+\pi^-$ decays. The $\pi^+\pi^-$ vertex is required to be displaced from the IP by a minimum transverse distance of 0.22 cm for high momentum (> 1.5 GeV/c) candidates and 0.08 cm for those with momentum less than 1.5 GeV/c. The direction of the pion pair momentum must also agree with the direction defined by the IP and the vertex displacement within 0.03 rad for high-momentum candidates, and within 0.1 rad for the remaining candidates. When we find two good K^{+-}_S candidates that satisfy the criteria described above, we apply looser selection criteria for the third K^{+-}_S candidate: (1) the mismatch in the z direction at the K^0_S vertex point for the two $\pi^\pm$ tracks should be less

than 5 cm (1cm when both pions have associated SVD hits); (2) the angle in the r-ϕ plane between the K^0_S momentum vector and the direction defined by the K^0_S and the IP should be less than 0.2 rad for high-momentum candidates, and less than 0.4 rad for the remaining candidates.

Photons are identified as isolated ECL clusters that are not matched to any charged track. To select $K^0_S \to \pi^0\pi^0$ decays, we reconstruct π^0 candidates from pairs of photons with $E_\gamma > 0.05$ GeV, where E_γ is the photon energy measured with the ECL. The reconstructed π^0 candidate is required to satisfy $0.08\ \mathrm{GeV}/c^2 < M_{\gamma\gamma} < 0.15\ \mathrm{GeV}/c^2$ and $p^{\rm cms}_{\pi^0} > 0.1$ GeV/c, where $M_{\gamma\gamma}$ and $p^{\rm cms}_{\pi^0}$ are the invariant mass and the momentum in the cms, respectively. The large mass range is used to achieve a high reconstruction efficiency. Candidate $K^0_S \to \pi^0\pi^0$ decays are required to have invariant masses between $0.47\ \mathrm{GeV}/c^2$ and $0.52\ \mathrm{GeV}/c^2$, where we perform a fit with constraints on the K^0_S vertex and the π^0 masses to improve the $\pi^0\pi^0$ invariant mass resolution. We also require that the distance between the IP and the reconstructed K^0_S decay vertex be between -10 cm and 100 cm, where the positive direction is defined by the K^0_S momentum. The K^{00}_S candidate is combined with two good K^{+-}_S candidates to reconstruct $B^0 \to K^{+-}_S K^{+-}_S K^{00}_S$ decay, where we only use aforementioned good K^{+-}_S candidates.

For reconstructed $B \to K^0_S K^0_S K^0_S$ candidates, we identify B meson decays using the energy difference $\Delta E \equiv E^{\rm cms}_B - E^{\rm cms}_{\rm beam}$ and the beam-energy constrained mass $M_{\rm bc} \equiv \sqrt{(E^{\rm cms}_{\rm beam})^2 - (p^{\rm cms}_B)^2}$, where $E^{\rm cms}_{\rm beam}$ is the beam energy in the cms, and $E^{\rm cms}_B$ and $p^{\rm cms}_B$ are the cms energy and momentum of the reconstructed B candidate, respectively. The B meson signal region is defined as $|\Delta E| < 0.10$ GeV for $B^0 \to K^{+-}_S K^{+-}_S K^{+-}_S$, $-0.15\ \mathrm{GeV} < \Delta E < 0.10$ GeV for $B^0 \to K^{+-}_S K^{+-}_S K^{00}_S$, and $5.27\ \mathrm{GeV}/c^2 < M_{\rm bc} < 5.29\ \mathrm{GeV}/c^2$ for both decays.

The dominant background to the $B^0 \to K^0_S K^0_S K^0_S$ decay comes from $e^+e^- \to u\overline{u}$, $d\overline{d}$, $s\overline{s}$, or $c\overline{c}$ continuum events. Since these tend to be jet-like, while the signal events tend to be spherical, we use a set of variables that characterize the event topology to distinguish between the two. We combine modified Fox-Wolfram moments [19] into a Fisher discriminant $\mathcal{F}$. We also use the angle of the reconstructed B^0 candidate with respect to the beam direction in the cms (θ_B). We combine $\mathcal{F}$ and $\cos\theta_B$ into a signal [background] likelihood variable, which is defined as $\mathcal{L}_{\rm sig[bkg]} \equiv \mathcal{L}_{\rm sig[bkg]}(\mathcal{F}) \times \mathcal{L}_{\rm sig[bkg]}(\cos\theta_B)$. We impose requirements on the likelihood ratio $\mathcal{R}_{\rm s/b} \equiv \mathcal{L}_{\rm sig}/(\mathcal{L}_{\rm sig} + \mathcal{L}_{\rm bkg})$ to maximize the figure-of-merit (FoM) defined as $N^{\rm MC}_{\rm sig}/\sqrt{N^{\rm MC}_{\rm sig} + N_{\rm bkg}}$, where $N^{\rm MC}_{\rm sig}$ ($N_{\rm bkg}$) represents the expected number of signal (background) events in the signal region. We estimate $N^{\rm MC}_{\rm sig}$ using Monte Carlo (MC) events, while $N_{\rm bkg}$ is determined from events outside the signal region. The requirement for $\mathcal{R}_{\rm s/b}$ depends both on the decay mode and on the flavor-tagging quality, r, which is described in Sec. II C. The threshold values range from 0.2 (used for $r > 0.875$) to 0.5 (used for $r < 0.25$) for the case with 3 good K^{+-}_S candidates, and from 0.3 to 0.9 for other cases.

We reject $K^0_S K^0_S K^0_S$ candidates that are consistent with $B^0 \to \chi_{c0} K^0_S \to (K^0_S K^0_S) K^0_S$ or $B^0 \to D^0 K^0_S \to (K^0_S K^0_S) K^0_S$. We keep candidate $B^0 \to f_0(980) K^0_S \to (K^0_S K^0_S) K^0_S$ decays as they are also dominated by the $b \to s$ transition.

We use events outside the signal region as well as a large MC sample to study the background components. The dominant background is from continuum. The contributions from $B\overline{B}$ events are small. The contamination of $B^0 \to \chi_{c0} K^0_S$ events in the $B^0 \to K^0_S K^0_S K^0_S$ sample is small (2.6%). The influence of this background is treated as a source of systematic uncertainty. Backgrounds from the decay $B^0 \to D^0 K^0_S$ are found to be negligible.

Figure 1(a) [(c)] shows the $M_{\rm bc}$ [ΔE] distribution for the reconstructed $B^0 \to K^0_S K^0_S K^0_S$ candidates within the ΔE [$M_{\rm bc}$] signal regions after flavor tagging and vertex reconstruction.

The signal yield is determined from an unbinned two-dimensional maximum-likelihood fit to the ΔE-$M_{\rm bc}$ distribution. The fit region for the $B^0 \to K^{+-}_S K^{+-}_S K^{+-}_S$ decay is defined as $5.20\ {\rm GeV}/c^2 < M_{\rm bc} < 5.30\ {\rm GeV}/c^2$ and $-0.30\ {\rm GeV} < \Delta E < 0.50\ {\rm GeV}$, excluding the region $5.26\ {\rm GeV}/c^2 < M_{\rm bc} < 5.30\ {\rm GeV}/c^2$ and $-0.30\ {\rm GeV} < \Delta E < -0.12\ {\rm GeV}$ to reduce the effect of background from B decays. The fit region for the $B^0 \to K^{+-}_S K^{+-}_S K^{00}_S$ decay is defined as $5.22\ {\rm GeV}/c^2 < M_{\rm bc} < 5.30\ {\rm GeV}/c^2$ and $-0.40\ {\rm GeV} < \Delta E < 0.40\ {\rm GeV}$, excluding the region $5.25\ {\rm GeV}/c^2 < M_{\rm bc} < 5.30\ {\rm GeV}/c^2$ and $-0.4\ {\rm GeV} < \Delta E < -0.17\ {\rm GeV}$. The $K^{+-}_S K^{+-}_S K^{+-}_S$ signal distribution is modeled with a Gaussian function (a sum of two Gaussian functions) for $M_{\rm bc}$ (ΔE). For the $B^0 \to K^{+-}_S K^{+-}_S K^{00}_S$ decay, the signal is modeled with a two-dimensional smoothed histogram obtained from MC events. For the continuum background, we use the ARGUS parameterization [20] for $M_{\rm bc}$ and a linear function for ΔE. The fits after flavor tagging yield 72 ± 10 $B^0 \to K^{+-}_S K^{+-}_S K^{+-}_S$ events and 16 ± 8 $B^0 \to K^{+-}_S K^{+-}_S K^{00}_S$ events for a total of 88 ± 13 $B^0 \to K^0_S K^0_S K^0_S$ events in the signal region, where the errors are statistical only.

B. $B^0 \to K^0_S \pi^0 \gamma$

Candidate $K^0_S \to \pi^+\pi^-$ decays are selected with the same criteria as those used to select good K^{+-}_S candidates for the $B^0 \to K^0_S K^0_S K^0_S$ decay, except that we impose a more stringent invariant mass requirement; only pairs of oppositely charged pions that have an invariant mass within $0.006\ {\rm GeV}/c^2$ of the nominal K^0_S mass are used. Candidate π^0 mesons are required to satisfy $0.118\ {\rm GeV}/c^2 < M_{\gamma\gamma} < 0.15\ {\rm GeV}/c^2$ and $p^{\rm cms}_{\pi^0} > 0.3\ {\rm GeV}/c$. The $K^0_S\pi^0$ invariant mass, $M_{K^0_S\pi^0}$, is required to be between 0.6 and $1.8\ {\rm GeV}/c^2$.

For prompt photons from the $B^0 \to K^0_S\pi^0\gamma$ decay, we select the photon with the largest $E^{\rm cms}_\gamma$ among photon candidates in an event and require $1.4\ {\rm GeV} < E^{\rm cms}_\gamma < 3.4\ {\rm GeV}$, where $E^{\rm cms}_\gamma$ is the photon energy in the cms. For the selected photon, we also require $E_9/E_{25} > 0.95$, where E_9/E_{25} is the ratio of energies summed in 3×3 and 5×5 arrays of CsI(Tl) crystals surrounding the crystal at the center of the shower. Photons for candidate $\pi^0 \to \gamma\gamma$ or $\eta \to \gamma\gamma$ decays are not used; we reject photon pairs that satisfy $\mathcal{L}_{\pi^0} \geq 0.18$ or $\mathcal{L}_\eta \geq 0.18$, where $\mathcal{L}_{\pi^0(\eta)}$ is a π^0 (η) likelihood described in detail elsewhere [21]. The polar angle of the photon direction in the laboratory frame is required to be between 33° and 128° for DS-I, while no requirement is imposed for DS-II as the material within the acceptance of the ECL is much reduced for this dataset.

Candidate $B^+ \to K^0_S\pi^+\gamma$ decays are also selected using a similar procedure to reconstruct the decay $B^0 \to K^0_S\pi^0\gamma$. Candidate $B^+ \to K^0_S\pi^+\gamma$ and $B^0 \to K^0_S\pi^0\gamma$ decays are selected simultaneously; we allow only one candidate for each event. The best candidate selection is based on the event likelihood ratio $\mathcal{R}_{\rm s/b}$ that is obtained by combining $\mathcal{F}$, which uses the extended modified Fox-Wolfram moments [22] as discriminating variables, with $\cos\theta_H$ defined as the angle between the B^0 meson momentum and the daughter K^0_S momentum in the rest frame of the $K^0_S\pi^0$ system. We select the candidate with the largest $\mathcal{R}_{\rm s/b}$.

The signal region for the $B^0 \to K^0_S\pi^0\gamma$ decay is defined as $-0.2\ {\rm GeV} < \Delta E < 0.1$ GeV, $5.27\ {\rm GeV}/c^2 < M_{\rm bc} < 5.29\ {\rm GeV}/c^2$. We require $\mathcal{R}_{\rm s/b} > 0.5$ to reduce the continuum background.

The selection criteria described above are the same as those used for the previous time-dependent CP asymmetry measurement in the $B^0 \to K^{*0}\gamma$ ($K^{*0} \to K^0_S\pi^0$) decay [10], except for the wider $M_{K^0_S\pi^0}$ range.

We use events outside the signal region as well as a large MC sample to study the background components. The dominant background is from continuum. Background contributions from B decays are significantly smaller than those from continuum, and are dominated by cross-feed from other radiative B decays including $B^+ \to K^0_S\pi^+\gamma$, and charmless B decays. Background from other $B\overline{B}$ decays is found to be negligible.

Figure 1(b) [(d)] shows the $M_{\rm bc}$ [ΔE] distribution for the reconstructed $B^0 \to K^0_S\pi^0\gamma$ candidates within the ΔE [$M_{\rm bc}$] signal region after flavor tagging and vertex reconstruction. The signal yield is determined from an unbinned two-dimensional maximum-likelihood fit to the ΔE-$M_{\rm bc}$ distribution in the fit region defined as 5.20 GeV/$c^2 < M_{\rm bc} <$ 5.29 GeV/c^2 and -0.4 GeV $< \Delta E <$ 0.5 GeV. The $B^0 \to K^0_S\pi^0\gamma$ signal distribution is represented by a smoothed histogram obtained from MC simulation that accounts for the correlation between $M_{\rm bc}$ and ΔE. The background from B decays is also modeled with a smoothed histogram obtained from MC events; its normalization is a free parameter in the fit. For the continuum background, we use the ARGUS parameterization for $M_{\rm bc}$ and a second-order Chebyshev function for ΔE. The fit yields 105 ± 14 $B^0 \to K^0_S\pi^0\gamma$ events, where the error is statistical only. For reference, we also measure the signal before vertex reconstruction and flavor tagging, and obtain 221 ± 21 events.

C. Flavor Tagging

The b-flavor of the accompanying B meson is identified from inclusive properties of particles that are not associated with the reconstructed $B^0 \to f_{CP}$ decay [23]. We use the same procedure that is used for the $\sin 2\phi_1$ measurement [5]. The algorithm for flavor tagging is described in detail elsewhere [24]. We use two parameters, q and r, to represent the tagging information. The first, q, is already defined in Eq. (1). The parameter r is an event-by-event, MC-determined flavor-tagging dilution factor that ranges from $r = 0$ for no flavor discrimination to $r = 1$ for unambiguous flavor assignment. It is used only to sort data into six r intervals. The wrong tag fractions for the six r intervals, w_l ($l = 1, 6$), and differences between B^0 and $\overline{B}^0$ decays, Δw_l, are determined from the data; we use the same values that were used for the $\sin 2\phi_1$ measurement [5] for DS-I. Wrong tag fractions for DS-II are separately obtained with the same procedure; we find that the values for DS-II, which are listed in Table I, are slightly smaller than those for DS-I. The total effective tagging efficiency for DS-II is determined to be $\epsilon_{\rm eff} \equiv \sum_{l=1}^{6} \epsilon_l (1 - 2w_l)^2 = 0.30 \pm 0.01$, where ϵ_l is the event fraction for each r interval determined from the $J/\psi K^0_S$ data and listed in Table I. The error includes both statistical and systematic uncertainties.

D. Vertex Reconstruction

The vertex position for $B^0 \to K^0_S K^0_S K^0_S$ and $B^0 \to K^0_S\pi^0\gamma$ decays is reconstructed using charged pions from K^0_S decays. A constraint on the IP is also used with the selected tracks; the IP profile is convolved with finite B flight length in the plane perpendicular to the z axis. Both charged pions from the K^0_S decay are required to have enough SVD hits to reconstruct a K^0_S trajectory with a sufficient resolution. The reconstruction efficiency depends both on the K^0_S momentum and on the SVD geometry. Efficiencies with SVD-II are higher than those with SVD-I because of the larger outer radius and the additional layer.

The $f_{\rm tag}$ vertex determination with SVD-I remains unchanged from the previous publication [10], and is described in detail elsewhere [25]; to minimize the effect of long-lived particles, secondary vertices from charmed hadrons and a small fraction of poorly reconstructed tracks, we adopt an iterative procedure in which the track that gives the largest contribution to the vertex χ^2 is removed at each step until a good χ^2 is obtained.

For SVD-II [10], we find that the same vertex reconstruction algorithm results in a larger outlier fraction when only one track remains after the iteration procedure. Therefore, in this case, we repeat the iteration procedure with a more stringent requirement on the SVD-II hit pattern. The resulting outlier fraction is comparable to that for SVD-I, while the inefficiency caused by this change is small (2.5%).

E. Summary of Signal Yields

The signal yields for $B^0 \to f_{CP}$ decays, $N_{\rm sig}$, after flavor tagging are summarized in Table II. For the $B^0 \to K^0_S K^0_S K^0_S$ decay, results both before and after vertex reconstruction are listed. The result for the $B^0 \to K^0_S \pi^0 \gamma$ is obtained after vertex reconstruction. The signal purities are also listed in the table.

III. RESULTS OF *CP* ASYMMETRY MEASUREMENTS

We determine $\mathcal{S}$ and $\mathcal{A}$ for each mode by performing an unbinned maximum-likelihood fit to the observed Δt distribution. The probability density function (PDF) expected for the signal distribution, $\mathcal{P}_{\rm sig}(\Delta t; \mathcal{S}, \mathcal{A}, q, w_l, \Delta w_l)$, is given by Eq. (1) incorporating the effect of incorrect flavor assignment. The distribution is convolved with the proper-time interval resolution function $R_{\rm sig}(\Delta t)$, which takes into account the finite vertex resolution.

The Δt resolution function for the $B^0 \to K^0_S \pi^0 \gamma$ decay is the same as that used in the previous analysis on the decay $B^0 \to K^{*0}\gamma$ ($K^{*0} \to K^0_S \pi^0$) [10]. It is based on the resolution function obtained from flavor-specific B decays governed by semileptonic or hadronic $b \to c$ transitions, with additional parameters that rescale vertex errors. The rescaling parameters depend on the detector configuration (SVD-I or SVD-II), SVD hit patterns of charged pions from the K^0_S decay, and K^0_S decay vertex position in the plane perpendicular to the beam axis. These parameters are determined from a fit to the Δt distribution of $B^0 \to J/\psi K^0_S$ data. Here the K^0_S and the IP constraint are used for the vertex reconstruction, the B^0 lifetime is fixed at the world average value, and b-flavor tagging information is not used so that the expected PDF is an exponential function convolved with the resolution function.

We check the resulting resolution function by also reconstructing the vertex with leptons from J/ψ decays and the IP constraint. We find that the distribution of the distance between the vertex positions obtained with the two methods is well represented by the obtained resolution function convolved with the well-known resolution for the J/ψ vertex. Finally, we also perform a fit to the $B^0 \to J/\psi K^0_S$ sample with b-flavor information and obtain $\mathcal{S}_{J/\psi K^0_S} = +0.68 \pm 0.10({\rm stat})$ and $\mathcal{A}_{J/\psi K^0_S} = +0.02 \pm 0.04({\rm stat})$, which are in good agreement with the world average values. Thus, we conclude that the vertex resolution for the $B^0 \to K^0_S \pi^0 \gamma$ decay is well understood.

The resolution function for the $B^0 \to K^0_S K^0_S K^0_S$ decay is based on the same resolution function parameterization. The rescaling factor depends on the detector configuration (SVD-I or SVD-II), SVD hit patterns of charged pions from the K^0_S decay, K^0_S decay vertex position

in the plane perpendicular to the beam axis, and the number of K_S^{+-} decays used for the vertex reconstruction.

We determine the following likelihood value for each event:

$$\begin{aligned} P_i &= (1-f_{\rm ol})\int\Big[f_{\rm sig}\mathcal{P}_{\rm sig}(\Delta t')R_{\rm sig}(\Delta t_i-\Delta t') \\ &+ (1-f_{\rm sig})\mathcal{P}_{\rm bkg}(\Delta t')R_{\rm bkg}(\Delta t_i-\Delta t')\Big]d(\Delta t') \\ &+ f_{\rm ol}P_{\rm ol}(\Delta t_i) \end{aligned} \tag{2}$$

where $P_{\rm ol}(\Delta t)$ is a broad Gaussian function that represents an outlier component with a small fraction $f_{\rm ol}$. The signal probability $f_{\rm sig}$ depends on the r region and is calculated on an event-by-event basis as a function of ΔE and $M_{\rm bc}$ for each mode. A PDF for background events, $\mathcal{P}_{\rm bkg}(\Delta t)$, is modeled as a sum of exponential and prompt components, and is convolved with a sum of two Gaussians $R_{\rm bkg}$. All parameters in $\mathcal{P}_{\rm bkg}(\Delta t)$ and $R_{\rm bkg}$ are determined by the fit to the Δt distribution of a background-enhanced control sample; i.e. events outside of the ΔE-$M_{\rm bc}$ signal region. We fix τ_{B^0} and Δm_d at their world-average values [26]. In order to reduce the statistical error on $\mathcal{A}$, we include events without vertex information in the analysis of $B^0 \to K_S^0K_S^0K_S^0$. The likelihood value in this case is obtained by integrating Eq. (2) over Δt_i.

The only free parameters in the final fit are $\mathcal{S}$ and $\mathcal{A}$, which are determined by maximizing the likelihood function $L = \prod_i P_i(\Delta t_i; \mathcal{S}, \mathcal{A})$ where the product is over all events.

Table III summarizes the fit results of $\mathcal{S}$ and $\mathcal{A}$. We define the raw asymmetry in each Δt bin by $(N_{q=+1} - N_{q=-1})/(N_{q=+1} + N_{q=-1})$, where $N_{q=+1(-1)}$ is the number of observed candidates with $q = +1(-1)$. Figures 2(a) and (b) show the raw asymmetries for the $B^0 \to K_S^0K_S^0K_S^0$ and $K_S^0\pi^0\gamma$ decays, respectively, in two regions of the flavor-tagging parameter r. While the numbers of events in the two regions are similar, the effective tagging efficiency is much larger and the background dilution is smaller in the region $0.5 < r \leq 1.0$. Note that these projections onto the Δt axis do not take into account event-by-event information (such as the signal fraction, the wrong tag fraction and the vertex resolution), which is used in the unbinned maximum-likelihood fit.

Table IV lists the systematic errors on $\mathcal{S}$ and $\mathcal{A}$. The total systematic errors are obtained by adding each contribution in quadrature, and are much smaller than the statistical errors for all modes.

To determine the systematic error that arises from uncertainties in the vertex reconstruction, the track and vertex selection criteria are varied to search for possible systematic biases. Small biases in the Δz measurement are observed in $e^+e^- \to \mu^+\mu^-$ and other control samples. Systematic errors are estimated by applying special correction functions to account for the observed biases, repeating the fit, and comparing the obtained values with the nominal results. The systematic error due to the IP constraint in the vertex reconstruction is estimated by varying ($\pm 10\mu$m) the smearing used to account for the B flight length. Systematic errors due to imperfect SVD alignment are determined from MC samples that have artificial mis-alignment effects to reproduce impact-parameter resolutions observed in data.

Systematic errors due to uncertainties in the wrong tag fractions are studied by varying the wrong tag fraction individually for each r region. Systematic errors due to uncertainties in the resolution function are also estimated by varying each resolution parameter obtained from data (MC) by $\pm 1\sigma$ ($\pm 2\sigma$), repeating the fit and adding each variation in quadrature.

Each physics parameter such as τ_{B^0} and Δm_d is also varied by its error. A possible fit bias is examined by fitting a large number of MC events.

Systematic errors from uncertainties in the background fractions and in the background Δt shape are estimated by varying each background parameter obtained from data (MC) by $\pm 1\sigma$ ($\pm 2\sigma$). Uncertainties in the background B decay model are also considered for the $B^0 \to K^0_S\pi^0\gamma$ mode; we compare different theoretical models for radiative B decays and take the largest variation as the systematic error.

Additional sources of systematic errors are considered for B decay backgrounds that are neglected in the PDF. We consider uncertainties both in their fractions and CP asymmetries; for modes that have non-vanishing CP asymmetries, we conservatively vary the CP-violation parameters within the physical region and take the largest variation as the systematic error. The effect of backgrounds from $\chi_{c0}K^0_S$ in the $B^0 \to K^0_S K^0_S K^0_S$ sample is considered.

Finally, we investigate the effects of interference between CKM-favored and CKM-suppressed $B \to D$ transitions in the $f_{\rm tag}$ final state [27]. A small correction to the PDF for the signal distribution arises from the interference. We estimate the size of the correction using the $B^0 \to D^{*-}\ell^+\nu$ sample. We then generate MC pseudo-experiments and make an ensemble test to obtain systematic biases in $\mathcal{S}$ and $\mathcal{A}$.

Various crosschecks of the measurement are performed. We reconstruct charged B meson decays that are the counterparts of the $B^0 \to f_{CP}$ decays and apply the same fit procedure. All results for the $\mathcal{S}$ term are consistent with no CP asymmetry, as expected. Lifetime measurements are also performed for the f_{CP} modes and the corresponding charged B decay modes. The fits yield τ_{B^0} and τ_{B^+} values consistent with the world-average values. MC pseudo-experiments are generated for each decay mode to perform ensemble tests. We find that the statistical errors obtained in our measurements are all consistent with the expectations from the ensemble tests.

A fit to the $B^0 \to K^0_S\pi^0\gamma$ subsample with $0.6 < M_{K^0_S\pi^0} < 0.8$ GeV/c^2 or $1.0 < M_{K^0_S\pi^0} < 1.8$ GeV/c^2, which excludes the K^{*0} mass region, yields $\mathcal{S} = -0.39^{+0.63}_{-0.52}$(stat) and $\mathcal{A} = +0.10 \pm 0.51$(stat). The result on the $\mathcal{S}$ term is consistent with the previous result obtained for the decay $B^0 \to K^{*0}\gamma$ ($K^{*0} \to K^0_S\pi^0$), $\mathcal{S} = -0.79^{+0.63}_{-0.50}$(stat) $\pm$ 0.10(syst), where $0.8 < M_{K^0_S\pi^0} < 1.0$ GeV/c^2 was required.

As discussed in Section I, to a good approximation, the SM predicts $\mathcal{S} = -\xi_f \sin 2\phi_1$ for the $B^0 \to K^0_S K^0_S K^0$ decay. Figure 3 summarizes the $\sin 2\phi_1$ determination based on Belle's $\mathcal{S}$ measurements using modes dominated by the $b \to s$ transition [10]. For each mode, the first error shown in the figure is statistical and the second error is systematic. We obtain $\sin 2\phi_1 = +0.39 \pm 0.11$ as a weighted average, where the error includes both statistical and systematic errors. The result differs from the SM expectation by 2.7 standard deviations.

IV. SUMMARY

We have performed a new measurement of CP-violation parameters for $B^0 \to K^0_S K^0_S K^0_S$ decay based on a sample of 275×10^6 $B\overline{B}$ pairs. The decay is dominated by the $b \to s$ flavor-changing neutral current and the $K^0_S K^0_S K^0_S$ final state is a CP eigenstate. Thus it is sensitive to a new CP-violating phase beyond the SM. The result differs from the SM expectation by 2.8 standard deviations. The combined result with the decays $B^0 \to \phi K^0$, $K^+K^-K^0_S$, $f_0(980)K^0_S$, $\eta' K^0_S$, ωK^0_S and $K^0_S\pi^0$, which are also dominated by the $b \to s$ transitions, differs from the SM expectation by 2.7 standard deviations.

We have also measured the time-dependent CP asymmetry in the decay $B^0 \to K^0_S\pi^0\gamma$, which is also sensitive to physics beyond the SM. The invariant mass of the $K^0_S\pi^0$ system is required to be between 0.6 and 1.8 GeV/c^2, which is an extension of the previous analysis performed with the decay $B^0 \to K^{*0}\gamma$ ($K^{*0} \to K^0_S\pi^0$). The statistical error is much reduced from the previous analysis by including more events, and the result is consistent with the previous analysis.

In both cases, measurements with a much larger data sample are required to conclusively establish the existence of a new CP-violating phase beyond the SM.

Acknowledgments

We thank the KEKB group for the excellent operation of the accelerator, the KEK Cryogenics group for the efficient operation of the solenoid, and the KEK computer group and the National Institute of Informatics for valuable computing and Super-SINET network support. We acknowledge support from the Ministry of Education, Culture, Sports, Science, and Technology of Japan and the Japan Society for the Promotion of Science; the Australian Research Council and the Australian Department of Education, Science and Training; the National Science Foundation of China under contract No. 10175071; the Department of Science and Technology of India; the BK21 program of the Ministry of Education of Korea and the CHEP SRC program of the Korea Science and Engineering Foundation; the Polish State Committee for Scientific Research under contract No. 2P03B 01324; the Ministry of Science and Technology of the Russian Federation; the Ministry of Education, Science and Sport of the Republic of Slovenia; the National Science Council and the Ministry of Education of Taiwan; and the U.S. Department of Energy.

---

[1] M. Kobayashi and T. Maskawa, Prog. Theor. Phys. **49**, 652 (1973).

[2] A. B. Carter and A. I. Sanda, Phys. Rev. D **23**, 1567 (1981); I. I. Bigi and A. I. Sanda, Nucl. Phys. **B193**, 85 (1981).

[3] Throughout this paper, the inclusion of the charge conjugate decay mode is implied unless otherwise stated.

[4] Belle Collaboration, K. Abe *et al.*, Phys. Rev. Lett. **87**, 091802 (2001); Phys. Rev. D **66**, 032007 (2002); Phys. Rev. D **66**, 071102 (2002).

[5] Belle Collaboration, K. Abe *et al.*, BELLE-CONF-0436, hep-ex/0408036.

[6] BaBar Collaboration, B. Aubert *et al.*, Phys. Rev. Lett. **89**, 201802 (2002).

[7] Heavy Flavor Averaging Group, http://www.slac.stanford.edu/xorg/hfag/.

[8] A. G. Akeroyd *et al.*, hep-ex/0406071 and references therein.

[9] See for example,
Y. Grossman and M. P. Worah, Phys. Lett. B **395**, 241 (1997); T. Moroi, Phys. Lett. B **493**, 366 (2000); D. Chang, A. Masiero and H. Murayama, Phys. Rev. D **67**, 075013 (2003); S. Baek, T. Goto, Y. Okada and K. i. Okumura, Phys. Rev. D **64**, 095001 (2001).

[10] Belle Collaboration, K. Abe *et al.*, hep-ex/0409049.

[11] T. Gershon and M. Hazumi, Phys. Lett. B **596**, 163 (2004).

[12] Belle Collaboration, A. Garmash *et al.*, Phys. Rev. D **69**, 012001 (2004).

[13] BaBar Collaboration, B. Aubert *et al.*, hep-ex/0408065.

[14] D. Atwood, M. Gronau and A. Soni, Phys. Rev. Lett. **79**, 185 (1997).
[15] D. Atwood, T. Gershon, M. Hazumi and A. Soni, hep-ph/0410036.
[16] S. Kurokawa and E. Kikutani *et al.*, Nucl. Instr. and Meth. A **499**, 1 (2003).
[17] Belle Collaboration, A. Abashian *et al.*, Nucl. Instr. and Meth. A **479**, 117 (2002).
[18] Y. Ushiroda (Belle SVD2 Group), Nucl. Instr. and Meth. A **511**, 6 (2003).
[19] Belle Collaboration, K. Abe *et al.*, Phys. Rev. Lett. **87**, 101801 (2001).
[20] ARGUS Collaboration, H. Albrecht *et al.*, Phys. Lett. B **241**, 278 (1990).
[21] Belle Collaboration, P. Koppenburg *et al.*, Phys. Rev. Lett. **93**, 061803 (2004).
[22] Belle Collaboration, K. Abe *et al.*, Phys. Rev. Lett. **91**, 261801 (2003).
[23] Possible f_{CP} states include $K^0_S\pi^0\gamma$ and $K^{*0}\gamma$ hereafter.
[24] H. Kakuno, K. Hara *et al.*, Nucl. Instr. and Meth. A **533**, 516 (2004).
[25] H. Tajima *et al.*, Nucl. Instr. and Meth. A **533**, 307 (2004).
[26] S. Eidelman *et al.*, Phys. Lett. B **592**, 1 (2004).
[27] O. Long, M. Baak, R. N. Cahn and D. Kirkby, Phys. Rev. D **68**, 034010 (2003).

TABLE I: The event fractions ϵ_l, wrong-tag fractions w_l, wrong-tag fraction differences Δw_l, and average effective tagging efficiencies $\epsilon^l_{\rm eff} = \epsilon_l(1-2w_l)^2$ for each r interval for the DS-II. The errors for w_l and Δw_l include both statistical and systematic uncertainties. The event fractions are obtained from $J/\psi K^0_S$ data.

l	r interval	ϵ_l	w_l	Δw_l	$\epsilon^l_{\rm eff}$
1	0.000 – 0.250	0.397 ± 0.015	0.464 ± 0.007	$+0.010 \pm 0.007$	0.002 ± 0.001
2	0.250 – 0.500	0.146 ± 0.009	0.321 ± 0.008	-0.022 ± 0.010	0.019 ± 0.002
3	0.500 – 0.625	0.108 ± 0.008	0.224 ± 0.011	$+0.031 \pm 0.011$	0.033 ± 0.004
4	0.625 – 0.750	0.107 ± 0.008	0.157 ± 0.010	$+0.002 \pm 0.011$	0.051 ± 0.005
5	0.750 – 0.875	0.098 ± 0.007	0.109 ± 0.009	-0.028 ± 0.011	0.060 ± 0.005
6	0.875 – 1.000	0.144 ± 0.009	0.016 ± 0.005	$+0.007 \pm 0.007$	0.135 ± 0.009

TABLE II: The estimated signal purity and the signal yield $N_{\rm sig}$ in the signal region for $B^0 \to K^0_S K^0_S K^0_S$ and $K^0_S\pi^0\gamma$ decays. For the $B^0 \to K^0_S K^0_S K^0_S$ decay, results both before and after vertex reconstruction (the latter in parentheses) are shown as events that do not have vertex information are also used to extract the direct CP violation parameter $\mathcal{A}$. For the $B^0 \to K^0_S\pi^0\gamma$ decay, the result after vertex reconstruction is shown.

Mode	purity	$N_{\rm sig}$
$K^0_S K^0_S K^0_S$	0.53 (0.54)	88 ± 13 (63 ± 9)
$K^{+-}_S K^{+-}_S K^{+-}_S$	0.56 (0.56)	72 ± 10 (54 ± 8)
$K^{+-}_S K^{+-}_S K^{00}_S$	0.40 (0.40)	16 ± 8 (8 ± 4)
$K^0_S\pi^0\gamma$	0.50	105 ± 14

TABLE III: Results of the fits to the Δt distributions. The first error is statistical and the second error is systematic.

Mode	SM expectation for $\mathcal{S}$	$\mathcal{S}$	$\mathcal{A}$
$K^0_S K^0_S K^0_S$	$-\sin 2\phi_1$	$+1.26 \pm 0.68 \pm 0.18$	$+0.54 \pm 0.34 \pm 0.08$
$K^0_S\pi^0\gamma$	$-2(m_s/m_b)\sin 2\phi_1$	$-0.58^{+0.46}_{-0.38} \pm 0.11$	$+0.03 \pm 0.34 \pm 0.11$

TABLE IV: Summary of the systematic errors on $\mathcal{S}$ and $\mathcal{A}$.

	$\mathcal{S}_{K^0_S K^0_S K^0_S}$	$\mathcal{S}_{K^0_S\pi^0\gamma}$	$\mathcal{A}_{K^0_S K^0_S K^0_S}$	$\mathcal{A}_{K^0_S\pi^0\gamma}$
Vertex reconstruction	0.02	0.05	0.05	0.06
Flavor tagging	0.04	0.01	0.01	0.01
Resolution function	0.12	0.05	0.04	0.04
Physics parameter	0.01	0.01	0.01	0.01
Possible fit bias	0.03	0.02	0.02	0.01
Background fraction	0.10	0.06	0.03	0.04
Background Δt shape	0.08	0.05	0.01	0.04
Tag-side interference	0.02	0.01	0.02	0.06
Total	0.18	0.11	0.08	0.11

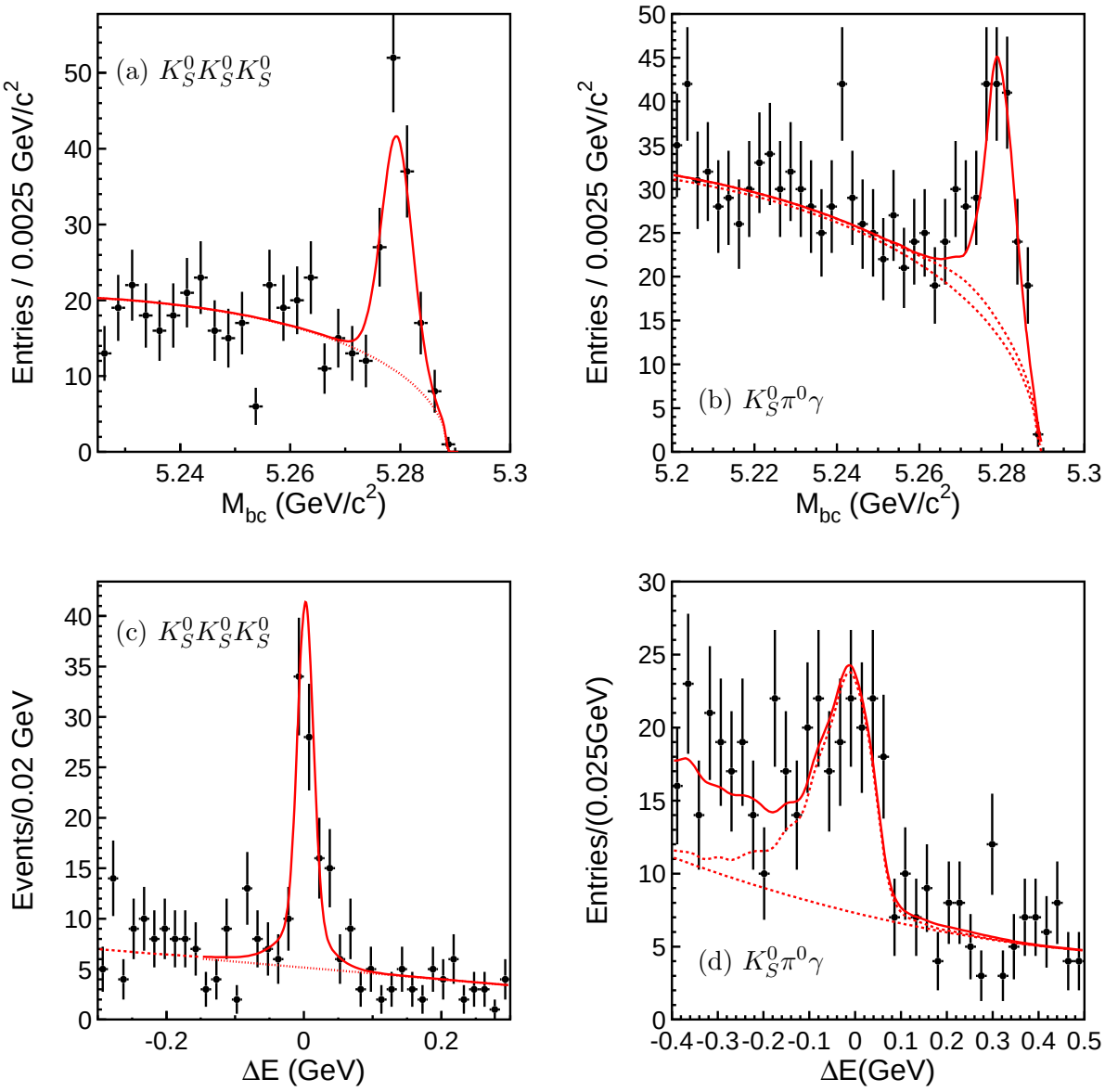

FIG. 1: The $M_{\rm bc}$ distributions within the ΔE signal region for (a) $B^0 \to K^0_S K^0_S K^0_S$ and (b) $B^0 \to K^0_S \pi^0 \gamma$, and the ΔE distributions within the $M_{\rm bc}$ signal region for (c) $B^0 \to K^0_S K^0_S K^0_S$ and (d) $B^0 \to K^0_S \pi^0 \gamma$. Solid curves show the fit to signal plus background distributions, and dashed curves show the background contributions.

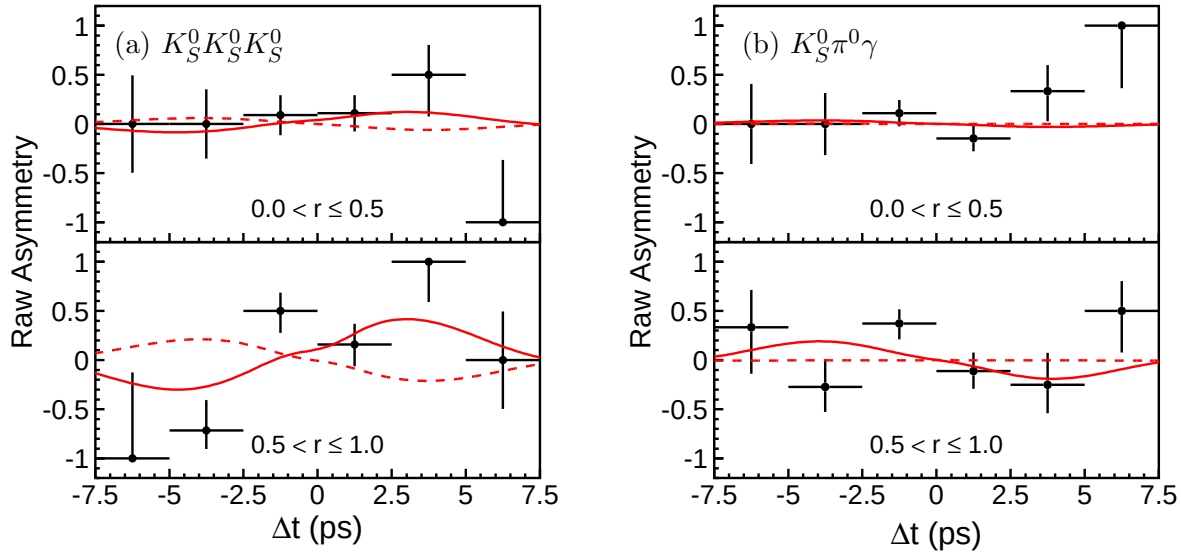

FIG. 2: The asymmetry, A, in each Δt bin with $0 < r \leq 0.5$ (top) and with $0.5 < r \leq 1.0$ (bottom) for (a) $B^0 \to K^0_S K^0_S K^0_S$ and (b) $B^0 \to K^0_S \pi^0 \gamma$. The solid curves show the result of the unbinned maximum-likelihood fit. The dashed curves show the SM expectation with $(\mathcal{S}, \mathcal{A}) = (-\sin 2\phi_1 = -0.73, 0)$ for $B^0 \to K^0_S K^0_S K^0_S$ and with $(\mathcal{S}, \mathcal{A}) = (0, 0)$ for $B^0 \to K^0_S \pi^0 \gamma$.

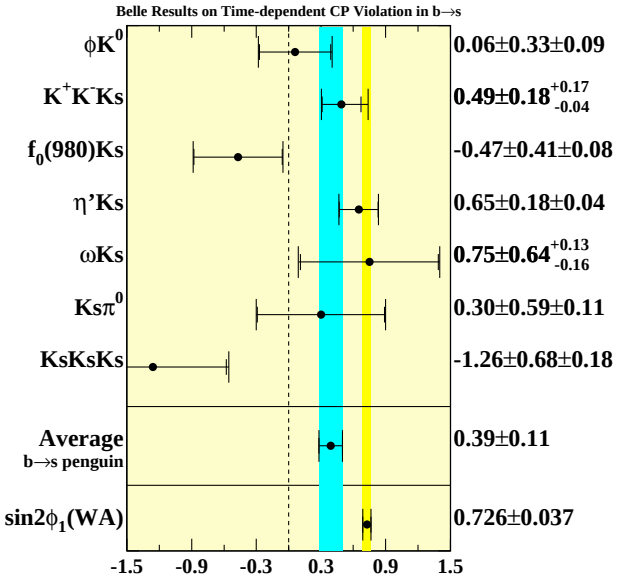

FIG. 3: Summary of $\sin 2\phi_1$ measurements performed with B^0 decay governed by the $b \to s\overline{q}q$ transition. The world-average $\sin 2\phi_1$ value obtained from $B^0 \to J/\psi K^0$ and other related decay modes governed by the $b \to c\overline{c}s$ transition [7] is also shown as the SM reference.